Pressure effect on the hydrogen vibrations in γ-TiH and γ-ZrH



2000 J. Phys.: Condens. Matter 12 4757

(http://iopscience.iop.org/0953-8984/12/22/308)

J. Phys.: Condens. Matter **12** (2000) 4757–4765. Printed in the UK PII: S0953-8984(00)11593-0

# Pressure effect on the hydrogen vibrations in $\gamma$-TiH and $\gamma$-ZrH

I O Bashkin†, A I Kolesnikov† and M A Adams‡

† Institute of Solid State Physics of the Russian Academy of Sciences, 142432, Chernogolovka, Moscow District, Russia

‡ The ISIS Facility, Rutherford Appleton Laboratory, Chilton, Didcot, Oxon OX11 0QX, UK

Received 3 February 2000, in final form 27 March 2000

**Abstract.** The inelastic neutron scattering spectra of $\gamma$-TiH and $\gamma$-ZrH were measured under high hydrostatic pressure. It was found that the energies of the hydrogen optical bands and bound multiphonon features (biphonons and triphonons) increased under pressure in linear proportion to their values at ambient pressure with the scaling factors of 1.02 for $\gamma$-TiH at $P = 15$ kbar and 1.03 for $\gamma$-ZrH at $P = 17.5$ kbar. The observed behaviour of the hydrogen-related spectral features is indicative of a uniform increase of the atomic force constants and the anharmonicity parameters in the model Hamiltonians representing the strength of two- and three-phonon interactions under pressure.

## 1. Introduction

There is a marked similarity between the $T$–$x$ phase diagrams of the Ti–H and Zr–H systems at atmospheric pressure [1–3]. Both diagrams involve the $\beta$–$(\alpha + \delta)$ eutectoid equilibrium at elevated temperatures and the $\delta$–$\varepsilon$ transformation in the dihydride phases. The $\alpha$- and $\beta$-phases are solid solutions of hydrogen in the hexagonal close-packed $\alpha$-Me and body-centred cubic Me sublattices, Me = Ti or Zr, whereas the dihydride phases, $\delta$-$MeH_{2-y}$ and $\varepsilon$-$MeH_{2-y}$, are formed on the basis of the face-centred cubic and face-centred tetragonal (axial ratio $c/a < 1$) metal sublattices, respectively. Hydrogen atoms in all these phases are randomly distributed on tetrahedral interstitial sites [1, 2, 4].

The fifth phase in these systems, monohydride $\gamma$-MeH, has also been reported to be stable at atmospheric pressure below 441 K in the Ti–H system [5] and below about 510 K in the Zr–H system [6]. The $\gamma$-MeH(D) phases have an ordered crystal structure where the hydrogen atoms occupy the tetrahedral interstitial sites (with unit-cell fractional coordinates $\frac{1}{4}\frac{3}{4}\frac{1}{4}$, $\frac{3}{4}\frac{1}{4}\frac{1}{4}$, $\frac{1}{4}\frac{3}{4}\frac{3}{4}$, $\frac{3}{4}\frac{1}{4}\frac{3}{4}$) on alternate [110] planes of the face-centred orthorhombic sublattice of the metal atoms with axial ratios $b/a \approx 1.015$ and $c/a \approx 1.09$ (space group $Cccm$) [4, 7, 8]. In these ordered structures, the H–H distance along crystal axis $c$ is shorter than that in the $ab$-plane by a factor of $\sqrt{2}/1.09 \simeq 1.3$, therefore the H–H interaction was discussed as essentially one dimensional.

The inelastic neutron scattering (INS) study of the vibrational spectra of these ordered phases demonstrated several unusual features [8–15]. A large dispersion was characteristic of the hydrogen optic vibrations so that the fundamental hydrogen bands were split into two ($\gamma$-TiH(D)) or three ($\gamma$-ZrH(D)) overlapping peaks. The other prominent feature of the spectra was their strong anharmonicity. All spectra showed a distinct peak below the band of the

0953-8984/00/224757+09$30.00  

harmonic two-phonon scattering and broader features below the third and fourth harmonic multiphonon bands. The anharmonic effects were discussed in terms of bound multiphonon states, i.e., biphonon, triphonon and tetraphonon excitations, as well as combined excitations involving biphonons or triphonons and free phonons.

The high-pressure behaviour of the anharmonic features has never been measured or predicted theoretically. This work presents the first experimental study of the effect of high hydrostatic pressure on the vibrational spectra of $\gamma$-TiH and $\gamma$-ZrH.

## 2. Experiment

An $(\alpha + \delta)$-$TiH_x$ alloy was prepared using a reaction of high-purity titanium ($\sim$99.98 at.%) with gaseous hydrogen obtained from thermally decomposed $TiH_2$ [3]. The hydrogen content was determined from the weight gain, $x = H/Ti = 0.76 \pm 0.01$. To eliminate any effect of crystal anisotropy, the sample was ground to about 0.3 mm particle size, then the powder was compacted into pellets of a 1 mm thickness. Further treatment of the sample involved high-pressure phase transformations. The sample was maintained at 670 K under a pressure of 65 kbar for 15 min, quenched to 80 K at a rate of about $10^3$ K $min^{-1}$ and recovered to ambient pressure under liquid nitrogen. The metastable phase thus obtained, $\chi$, transforms upon heating to room temperature to a two-phase state consisting of bulk stoichiometric $\gamma$-TiH and fine-grained $\tilde{\alpha}$-Ti precipitates with a grain size of about 100 Å [4, 16]. The hydrogen content in the $\tilde{\alpha}$-Ti precipitates is close to zero below room temperature [4], as was the case for the $\alpha$-phase [1]. So, the prepared sample consisted of $\gamma$-TiH and $\tilde{\alpha}$-Ti, and the latter phase did not contribute to the INS spectra in the range of the hydrogen optical modes.

The $(\alpha + \delta)$-$ZrH_x$ alloy, $x = H/Zr = 0.68 \pm 0.01$, was prepared in a similar way using metal Zr of $\sim$99.96 at.% purity. The $\gamma$-phase formation in the Zr–H system is facilitated compared to the Ti–H system therefore the $\delta$-phase in this sample completely transformed to $\gamma$-ZrH after room temperature ageing for about ten years. So, the phase composition of the present $ZrH_{0.68}$ sample was $\alpha$-Zr + $\gamma$-ZrH [12] with the $\alpha$-phase that did not contribute to the hydrogen optic vibrations. The $ZrH_{0.68}$ ingot was spark cut to 0.6 mm thick plates.

Hydrostatic pressure was generated using a clamped piston–cylinder device of the McWhan design with a hydrogen free pressure-transmitting fluid (Fluorinert FC-75) to ensure hydrostaticity. The technique is described in detail elsewhere [17, 18]. INS measurements were carried out at 25 K using the time-focused crystal analyser (TFXA) spectrometer [19] at the spallation neutron source, ISIS, Rutherford Appleton Laboratory, UK. The spectrometer provided an excellent energy resolution, $\Delta\omega/\omega \leqslant 2\%$, in the range of energy transfer 2 to 500 meV. The data were transformed to dynamical structure factor $S(Q, \omega)$ against energy transfer $\omega$ using standard programs. The background from the empty high-pressure cell in the cryostat was measured under the same experimental conditions and subtracted from the experimental data.

## 3. Results and discussion

The experimental INS spectrum from $(\tilde{\alpha} + \gamma)$-$TiH_{0.76}$ at $P = 15$ kbar is compared in figure 1 with the $(\tilde{\alpha} + \gamma)$-$TiH_{0.74}$ spectrum measured at atmospheric pressure earlier [11]. A similar comparison of the INS spectra from $((\alpha + \gamma)$-$ZrH_{0.68}$ at $P = 17.5$ kbar and $P = 1$ atm [12] is presented in figure 2. A strong resemblance of the spectral features is obvious in each figure both in the range of the fundamental band (140 to 180 meV) and in the range of the multiphonon excitations (above 260 meV). The main effect of applied pressure is a shift of all bands to higher energies.

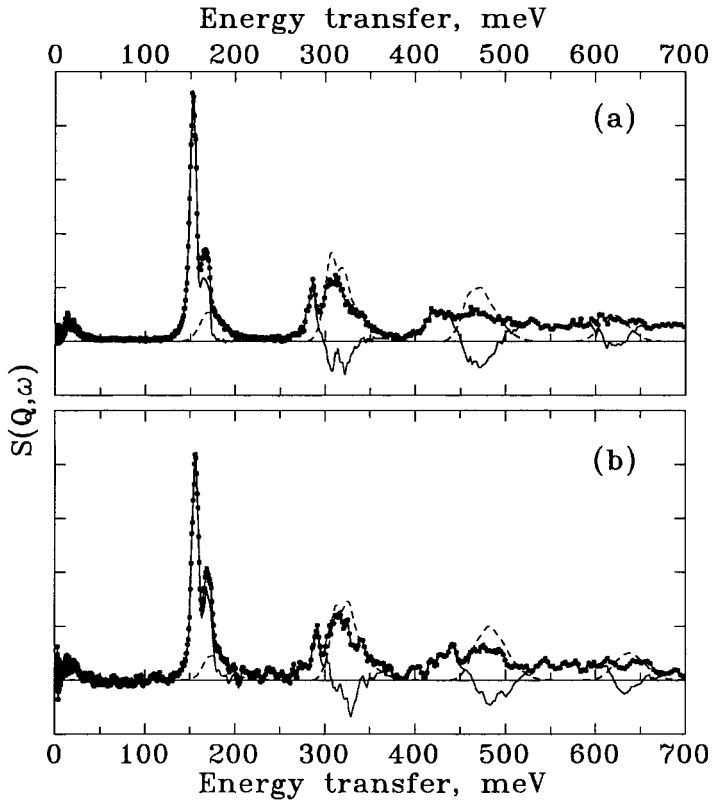


**Figure 1.** The INS spectra, $S(Q, \omega)$, from $\tilde{\alpha}$-Ti + $\gamma$-TiH at atmospheric pressure and $T = 95$ K [11, 13] (a) and at $P = 15$ kbar and $T = 25$ K (b). The experimental data are plotted with circles, the calculated multiphonon contributions are shown in dashed curves and the solid curves represent the difference between the experimental data and the calculated multiphonon spectrum.

The pressure effect on the low-energy part of the spectrum where the lattice vibrations are mainly determined by the dynamics of the heavier metal atoms is illustrated in figure 3 for the case of the Ti–H alloy. In spite of a lower statistics of the high-pressure spectrum, it is seen that the spectra measured at $P = 1$ atm and $P = 15$ kbar are similarly shaped. The intensities of the main spectral features are much the same at both pressures, the position of the acoustic peak at about 13.5 meV is not changed and the shifts of other lattice features are small and do not show a regular behaviour (the largest shift is about 1 meV for the peak around 20 meV). For the $ZrH_{0.68}$ alloy, the pressure effect in the range of lattice vibrations was also small. The low-energy ranges of the spectra were used in the present work only for calculation of the multiphonon neutron scattering and are not discussed in more detail.

The total range of the one-phonon spectrum was assumed to be 2 to 180 meV (see figures 1 and 2). The contribution from multiphonon neutron scattering was calculated in the harmonic isotropic approximation up to four-phonon processes. The iterative procedure based on multiconvolution of the one-phonon spectrum was described in rather detail previously [8, 9, 12]. The calculation results are shown in figures 1 and 2 where the contributions from the harmonic multiphonon neutron scattering are plotted as dashed curves and the solid curves represent the difference between the experimental and calculated multiphonon spectra. The solid curves

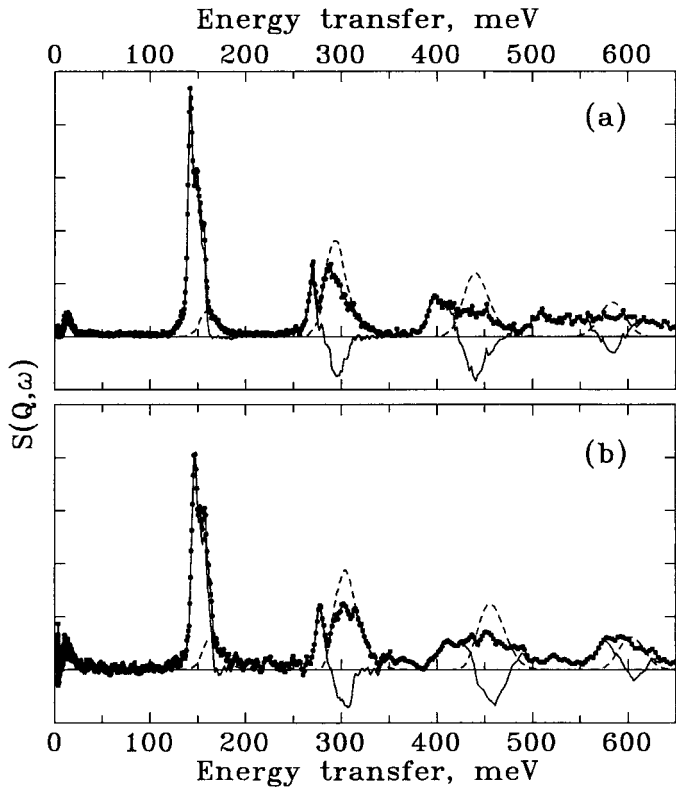


**Figure 2.** The INS spectra, $S(Q, \omega)$, from $\alpha$-Zr + $\gamma$-ZrH at atmospheric pressure and $T = 4.5$ K [12] (a) and from the same sample at $P = 17.5$ kbar and $T = 25$ K (b). Designations are the same as in figure 1.

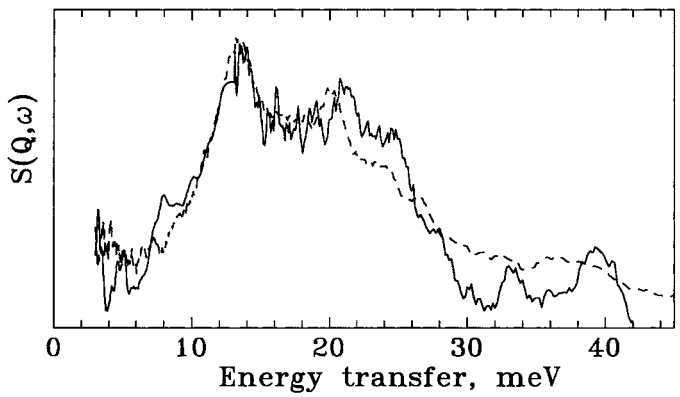


**Figure 3.** Lattice vibrations in the INS spectra from the ($\tilde{\alpha}$-Ti + $\gamma$-TiH) sample studied at atmospheric pressure and $T = 95$ K [11, 13] (dashed line) and at $P = 15$ kbar and $T = 25$ K (solid line).

below 180 meV present the calculated one-phonon spectra. Anharmonicity of the spectra is distinctly observed in the difference curves above 260 meV as the intensity deficit in the harmonic multiphonon bands and strong features due to bound multiphonons below the harmonic bands.

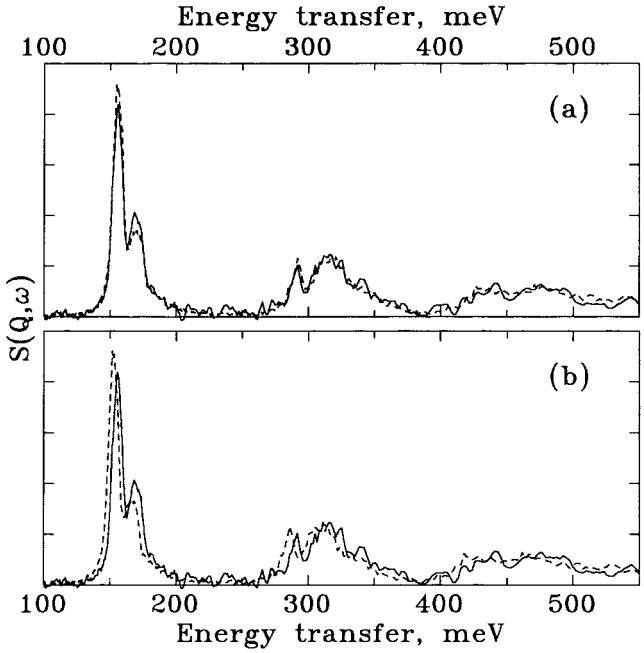


**Figure 4.** Superposition of the hydrogen vibrational spectra in $\gamma$-TiH at $P = 15$ kbar and $P = 1$ atm (solid and dashed curves, respectively): (a) the spectrum at atmospheric pressure is scaled up in energy by a factor of 1.02, (b) on the natural scale.

The hydrogen vibrational spectra of $\gamma$-TiH at ambient pressure and at $P = 15$ kbar are directly compared in figure 4. Their superposition is presented in figure 4(b), and figure 4(a) shows that the high-pressure spectrum can be well reproduced by the spectrum at ambient pressure by means of scaling up of the energy axis of the latter by a factor of 1.02. A good correspondence of the curves in figure 4(a) is indicative of a pressure-induced increase in the H–H force constants by about 4%. This increase is reasonable because the lattice contraction under pressure should result in stiffening of the interatomic interaction. The fact that anharmonic features follow the behaviour of the fundamental lines could hardly be anticipated.

The superposition of the spectra demonstrates also a re-distribution of the relative intensity in the hydrogen fundamental band. As a result, the relative intensity of the high-energy line increased compared to the low-energy one. To make a comparison, the fundamental band in the $\gamma$-TiH high-pressure spectrum was described with the Gaussian functions. The adequate accuracy of fitting was obtained using three Gaussians with the parameters listed in table 1 together with the earlier data [10]. It is seen from the table that two main lines are shifted under high pressure by the same value of 3.3 meV. The third fitting Gaussian appears as a broad low-intensity background under the main band.

Anharmonic features in the INS spectrum of $\gamma$-TiH are shown in more detail in figure 5 where the spectral intensity in the range of two- and three-phonon processes is scaled up by a factor of 3. A sharp peak of bound biphonon states is observed near 290 meV, well below the harmonic two-phonon band. The parameters of the fitting Gaussian (solid line in the right part) are presented in table 1. In the range of three-phonon processes, high scattering intensity at 410 to 450 meV evidences occurrence of bound multiphonon states, but a more detailed

**Table 1.** Peak positions, full widths at half maximum and intensities of Gaussians fitting the hydrogen optical vibrational bands in the INS spectra of $\gamma$-TiH and $\gamma$-ZrH at indicated pressures. Symbols $\omega_i$, $E_i$ and $\omega_{anh}$ are used, respectively, for the lines in the one-phonon bands, for the bound multiphonon excitations and for the simulated 'anharmonicity' peaks (see text).

| | TiH, 1 atm [10, 13] | TiH, 15 kbar | ZrH, 1 atm [12] | ZrH, 17.5 kbar |
|---|---|---|---|---|
| $\omega_1$ (meV) | 152.7 | 155.8 | 141.6 | 146.8 |
| $\Delta\omega_1$ (meV) | 9.0 | 8.1 | 5.5 | 7.8 |
| Int. (a.u.) | 0.776 | 0.518 | 0.444 | 0.400 |
| $\omega_2$ (meV) | 166.7 | 169.7 | 148.8 | 152.3 |
| $\Delta\omega_2$ (meV) | 10.2 | 10.7 | 7.8 | 2.8 |
| Int. (a.u.) | 0.224 | 0.299 | 0.416 | 0.329 |
| $\omega_3$ (meV) | | 153.2 | 156.0 | 156.7 |
| $\Delta\omega_3$ (meV) | | 19.1 | 5.4 | 7.1 |
| Int. (a.u.) | | 0.183 | 0.140 | 0.227 |
| $\omega_4$ (meV) | | | | 163.0 |
| $\Delta\omega_4$ (meV) | | | | 4.5 |
| Int. (a.u.) | | | | 0.044 |
| $E_2$ (meV) | 285.5 | 290.2 | 269.7 | 277.3 |
| $\Delta E_2$ (meV) | 9.8 | 9.9 | 6.7 | 10.2 |
| Int. (a.u.) | | 0.177 | | 0.156 |
| $E_3$ (meV) | 423.3 | | 397.0 | 408.2 |
| $\Delta E_3$ (meV) | 25.0 | | 13.3 | 20.8 |
| Int. (a.u.) | | | | 0.147 |
| $E_4$ (meV) | 530.0 | | 508.0 | |
| $\Delta E_4$ (meV) | 13.0 | | 21.0 | |
| $\omega_{anh}$ (meV) | 160.4 | 163.0 | 149.0 | 153.2 |
| $\Delta\omega_1$ (meV) | 20.0 | 20.0 | 10.0 | 10.0 |
| Int. (a.u.) | 0.184 | 0.256 | 0.210 | 0.187 |

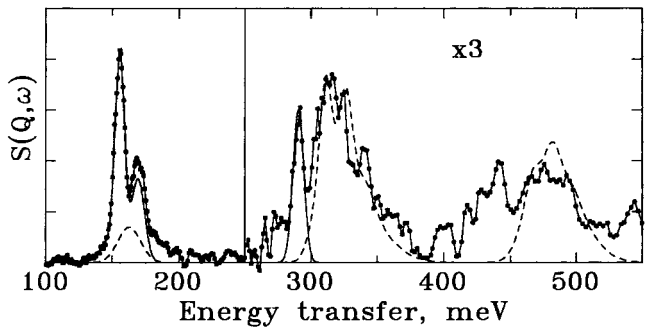


**Figure 5.** The hydrogen vibrational spectrum of $\gamma$-TiH at $P = 15$ kbar. The left part presents the experimental points, the calculated one-phonon spectrum (solid curve) and the peak of hydrogen vibrational states that involved into phonon binding (dashed curve). The right part (scaled by 3 times) shows the experimental points in the range of two- and three-phonon neutron scattering, the peak of bound biphonon states (solid curve) and the harmonic multiphonon bands (dashed curve) calculated from the one-phonon spectrum reduced by the peak presented in the left part.

discussion of these states is not reasonable because the statistics of the high-pressure spectrum is not sufficient between 400 and 500 meV.

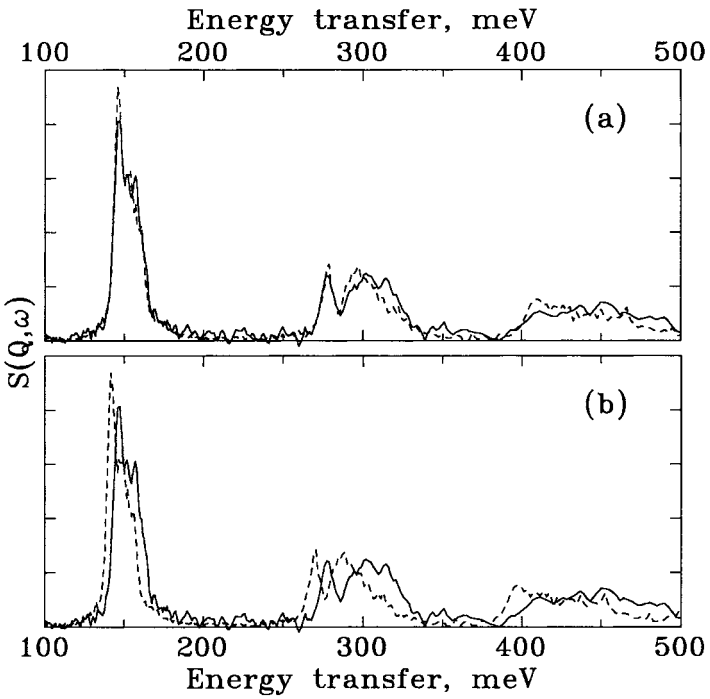


**Figure 6.** Superposition of the hydrogen vibrational spectra of $\gamma$-ZrH at $P = 17.5$ kbar and $P = 1$ atm (solid and dashed curves, respectively): (a) the spectrum at atmospheric pressure is scaled up in energy by a factor of 1.03, (b) on the natural scale.

The part of the one-phonon states involved in phonon binding was estimated following the procedure introduced previously [12, 13]. For this purpose, the hydrogen fundamental band was modified to fit the harmonic part of the multiphonon bands. A good agreement between the experimental points and the calculated harmonic multiphonon bands (plotted in dashed lines in the right part of figure 5) was obtained when the hydrogen fundamental band was reduced by a Gaussian peak shown in a dashed line in the left part of figure 5. The parameters of this 'anharmonicity' peak are presented in table 1.

A similar consideration of the hydrogen vibrational spectrum of $\gamma$-ZrH at $P = 17.5$ kbar is represented in figures 6 and 7. Figure 6(a) demonstrates that the positions of the main hydrogen related features in the high-pressure spectrum coincide with those in the $\gamma$-ZrH spectrum taken at $P = 1$ atm and scaled up in energy by a factor of 1.03. The magnitude of scaling corresponds to a pressure-induced increase in the H–H force constants by about 6%. A re-distribution of the relative intensity in the hydrogen fundamental band under pressure is the case for $\gamma$-ZrH as well. The fundamental band in the $\gamma$-ZrH spectrum at $P = 1$ atm has been described earlier [12] as a sum of three Gaussian lines. On the basis of the Born–von Kárman model calculation [12], the low-energy line was attributed to hydrogen vibrations in the *ab*-plane, the high-energy line was due to hydrogen vibrations along the *c*-axis, and both kinds of vibrational mode contributed to the intermediate peak. It is seen from figure 6(b) that the intensity of the high-energy line increased and that of the low-energy line decreased at $P = 17.5$ kbar. The fundamental band in the present $\gamma$-ZrH spectrum at $P = 17.5$ kbar was described using four fitting Gaussians, their parameters are listed in table 1 together with the data for $P = 1$ atm [12]. A larger number of fitting Gaussians is an indication that the

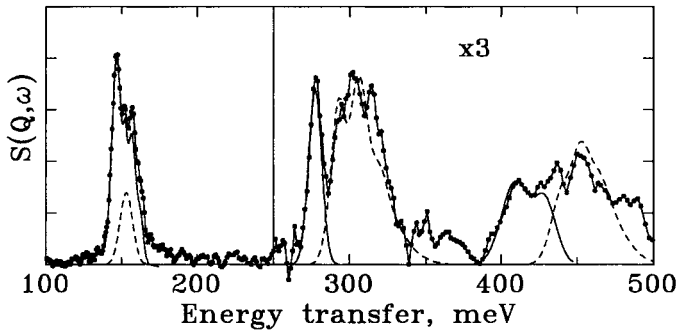


**Figure 7.** The hydrogen vibrational spectrum of $\gamma$-ZrH at $P = 17.5$ kbar. The left part presents the experimental points, the calculated one-phonon spectrum (solid curve) and the peak of hydrogen vibrational states that involved in phonon binding (dashed curve). The right part (scaled by 3 times) shows the experimental points in the range of two- and three-phonon neutron scattering, peaks of bound multiphonon states (solid curves) and the harmonic multiphonon bands (dashed curves) calculated from the one-phonon spectrum reduced by the peak presented in the left part.

dispersion of the hydrogen vibrational modes can be more complex than assumed in [12], at least, under high pressure.

Anharmonic contributions to the multiphonon neutron scattering processes in $\gamma$-ZrH are considered in figure 7. The peak of the bound biphonon excitations at 277.3 meV is distinct again, and the spectrum statistics is sufficient in order to determine the positions of the triphonon and biphonon + one-phonon peaks. The 'anharmonicity' peak for the $\gamma$-ZrH spectrum is shown as a dashed curve in the left part of figure 7. Subtraction of this peak from the one-phonon spectrum (solid curve) provides a better description of the harmonic multiphonon bands (dashed curves in the right part), as in the case of $\gamma$-TiH. So, the part of the hydrogen optical vibrations under the 'anharmonicity' peak is assumed to be involved in phonon binding. The parameters of the anharmonic features in the $\gamma$-ZrH spectrum are also listed in table 1.

The energies of the anharmonic features in the optical spectra have been parametrized within the theory of bound multiphonons using the following simple expressions [20, 21]

$$E_2 = 2\omega' - 2A \qquad \text{and} \qquad E_3 = 3\omega' - 6(A + \tilde{A}) \tag{1}$$

where $\omega'$ is the frequency of the hydrogen optical mode and anharmonicity constants $A$ and $\tilde{A}$ are coefficients at the quadratic and cubic terms of the model Hamiltonian representing the strength of the two- and three-particle interactions. The observed uniform linear shifts of all vibrational features in the spectra under high pressure suggest that the anharmonicity constants $A$ and $\tilde{A}$ increase under high pressure by the same factor as the energies of the one-phonon states involved in phonon binding. The anharmonicity constants $A$ and $\tilde{A}$ can be easily calculated from the data in table 1 under the assumption that $\omega' = \omega_{anh}$. The increase in their absolute values under pressure by 1.5 to 2.9% supports the latter conclusion.

## 4. Conclusions

This is the first experimental study of the pressure effect on the bound multiphonon states in metal hydrides. High hydrostatic pressure of 15–17.5 kbar results in hardening of the hydrogen optic vibrations in $\gamma$-TiH and $\gamma$-ZrH and a re-distribution of the scattering intensity between the one-phonon optical modes. The bound multiphonon features undergo an energy shift under high pressure that is approximately multiple to the shift of the one-phonon excitations. This

indicates that the parameters of the phonon–phonon interaction increase under high pressure in the same proportion as the energies of the one-phonon states.

## Acknowledgments

The authors are grateful to Professor V G Glebovsky for preparation of pure Ti and Zr and to Professor E G Ponyatovsky for useful discussion of the manuscript. We also thank ISIS for provision of the neutron beam facilities. The work was supported by the RFBR grants No 97-02-17614 and No 96-15-96806.

## References

[1] San-Martin A and Manchester F D 1987 *Bull. Alloy Phase Diagrams* **8** 30–42
San-Martin A and Manchester F D 1987 *Bull. Alloy Phase Diagrams* **8** 81–2
[2] Zuzek E, Abriata J P, San-Martin A and Manchester F D 1990 *Bull. Alloy Phase Diagrams* **11** 385–95
Zuzek E, Abriata J P, San-Martin A and Manchester F D 1990 *Bull. Alloy Phase Diagrams* **11** 2078–80
[3] Bashkin I O, Gurov A F, Malyshev V Yu and Ponyatovsky E G 1992 *Sov. Phys.–Solid State* **34** 674–80
[4] Kolesnikov A I, Balagurov A M, Bashkin I O, Fedotov V K, Malyshev V Yu, Mironova G M and Ponyatovsky E G 1993 *J. Phys.: Condens. Matter* **5** 5045–58
[5] Bashkin I O, Malyshev V Yu and Ponyatovsky E G 1993 *Z. Phys. Chem.* **179** 111–7
[6] Bashkin I O, Malyshev V Yu and Ponyatovsky E G 1993 *Z. Phys. Chem.* **179** 289–99
[7] Balagurov A M, Bashkin I O, Kolesnikov A I, Malyshev V Yu, Mironova G M, Ponyatovsky E G and Fedotov V K 1991 *Sov. Phys.–Solid State* **33** 711–14
[8] Kolesnikov A I, Balagurov A M, Bashkin I O, Belushkin A V, Ponyatovsky E G and Prager M 1994 *J. Phys.: Condens. Matter* **6** 8977–88
[9] Kolesnikov A I, Prager M, Tomkinson J, Bashkin I O, Malyshev V Yu and Ponyatovskii E G 1991 *J. Phys.: Condens. Matter* **3** 5927–36
Kolesnikov A I, Prager M, Tomkinson J, Bashkin I O, Malyshev V Yu and Ponyatovskii E G 1991 *J. Phys.: Condens. Matter* **3** 8015
[10] Kolesnikov A I, Bashkin I O, Malyshev V Yu, Ponyatovsky E G, Prager M and Tomkinson J 1992 *Physica* B **180/181** 284–6
[11] Bashkin I O, Kolesnikov A I, Malyshev V Yu, Ponyatovsky E G, Prager M and Tomkinson J 1993 *Z. Phys. Chem.* **179** 335–42
[12] Kolesnikov A I, Bashkin I O, Belushkin A V, Ponyatovsky E G and Prager M 1994 *J. Phys.: Condens. Matter* **6** 8989–9000
[13] Bashkin I O, Kolesnikov A I and Ponyatovsky E G 1995 *High Pressure Res.* **14** 91–100
[14] Kolesnikov A I, Bashkin I O, Belushkin A V, Ponyatovsky E G, Prager M and Tomkinson J 1995 *Physica* B **213/214** 445 –7
[15] Kolesnikov A I, Bashkin I O, Ponyatovsky E G, Prager M and Belushkin A V 1995 *Neutron Scattering in Materials Science II, Proc. 1994 MRS Fall Meeting* vol 376, ed D A Neumann, T P Russell and B J Wuensch (Pittsburg, PA: Materials Research Society) pp 733–8
[16] Bashkin I O, Kolesnikov A I, Malyshev V Yu, Ponyatovsky E G, Borbely S, Rosta L and Pepy G 1993 *J. Physique Coll.* IV **3** C8 287–90
[17] Adams M A and Tomkinson J 1992 *Physica* B **180/181** 694–6
[18] Adams M A 1995 *High Pressure Res.* **14** 21–7
[19] Penfold J and Tomkinson J 1986 *Rutherford Appleton Laboratory Report* RAL-86-019
[20] Agranovich V M, Dubovskii O A and Orlov A V 1986 *Phys. Lett.* A **119** 83
[21] Agranovich V M and Dubovskii O A 1986 *Rev. Phys. Chem.* **5** 93